

Hybrid LQG-Neural Controller for Inverted Pendulum System

E.S. Sazonov

Department of Electrical and Computer Engineering
Clarkson University
Potsdam, NY 13699-5720 USA

P. Klinkhachorn and R. L. Klein

Lane Dept. of Computer Science and Electrical Engineering,
West Virginia University,
Morgantown, WV 26506-6109 USA

Keywords: system controller, neural networks, hybrid controller, inverted pendulum

Abstract — The paper presents a hybrid system controller, incorporating a neural and an LQG controller. The neural controller has been optimized by genetic algorithms directly on the inverted pendulum system. The failure-free optimization process stipulated a relatively small region of the asymptotic stability of the neural controller, which is concentrated around the regulation point. The presented hybrid controller combines benefits of a genetically optimized neural controller and an LQG controller in a single system controller. High quality of the regulation process is achieved through utilization of the neural controller, while stability of the system during transient processes and a wide range of operation are assured through application of the LQG controller. The hybrid controller has been validated by applying it to a simulation model of an inherently unstable system – inverted pendulum.

I. INTRODUCTION

The traditional approach to building system controllers requires a prior model of the system. The quality of the model, that is, loss of precision from linearization and/or uncertainties in the system's parameters negatively influence the quality of the resulting control.

At the same time, methods of soft computing such as neural networks or fuzzy logic possess non-linear mapping capabilities, do not require an analytical model and can deal with uncertainties in the system's parameters. Combined with the evolutionary learning (such as genetic algorithms) these methods are capable of producing near-optimal controllers for a given control task. For example, genetic algorithms have been used to produce parameters of an optimized system controller such as the architecture and/or weights of a neural network controller [1,2], rules and/or membership functions of a fuzzy controller [3,4], and to obtain model equations [5], etc.

The disadvantage of the Genetic Algorithms (GA) is that the process routinely produces solutions (parameter sets of a controller) that may render the controlled system unstable.

A failure-free optimization method employing GA and a neural controller has been described in [6]. The suggested method applies evolutionary learning to a neural controller in

a subspace around the regulation point to ensure a failure-free optimization process. Thus, due to the nature of the failure-free learning methodology, the optimized neural controller is capable of controlling the system in a relatively small region of state space, which may be a limiting factor for some practical applications of the optimized neural controller.

This paper presents a hybrid controller that combines the benefits of an optimized neural controller and an LQG controller in a single system controller. The high quality of regulation process is ensured by application of the optimized neural controller, while the wide range of operation and stability of transient processes is provided by the LQG controller.

II. TEST BED

A numerical model of an Inverted Pendulum (IP) served as the test bed for the development of the proposed hybrid controller. Utilization of a model instead of an actual system allowed expediting and simplifying the experimentation process. The performance and accuracy of the model was verified during the design of the LQG controller [7].

The IP system consists of a cart sliding on a rail and a rod pivoted to the cart and free to rotate about an axis perpendicular to the direction of motion of the cart. The system is equipped with two sensors measuring cart position and rod angle, and a DC motor providing actuation control. The numerical model of the IP system not only simulates the dynamics of IP motion, including saturations on the state variables of cart position and rod angle, but also accounts for major non-linearities of the system, including the dead zone and saturation of the DC motor input voltage and force it can produce. Additionally, the model incorporates such parameters as sensor offsets, discretization errors and measurement noise. More details of the model, including corresponding modeling equations can be found in [7].

III. EXPERIMENTAL SETUP

This paper describes a hybrid controller that utilizes a neural and an LQG controller. The block diagram of the hybrid controller is presented in Fig. 1. The numerical model described in section II simulates an inverted pendulum

system. A linearized model of the IP dynamics was adopted for the purpose of designing the LQG controller:

$$\begin{cases} (M+m)\ddot{p}(t) + m\frac{l}{2}\ddot{\Theta}(t) = C_V V(t) - (C_p + \beta)\dot{p}(t) \\ -m\frac{l}{2}\ddot{\Theta}(t) = m\dot{p}(t) \end{cases}, \quad (1)$$

where M and m are rod and cart masses respectively, l is the rod length, $p(t)$ is the cart position with respect to the center of the rail, $\Theta(t)$ is the rod angle with respect to the vertical, C_V is the motor torque constant, $V(t)$ is the voltage supplied to the electric motor, C_p and β are the coefficients reflecting the dynamic and static friction in the coupling between the motor shaft and the rail. A detailed description of the LQG controller can be found in [7].

The neural controller is a multi-layer perceptron (neural network) composed of the neurons with the sigmoid transfer function. The neural controller has a fixed architecture:

- Four inputs – cart position in meters (from -0.5 to 0.5 with respect to the center of the rail); cart velocity in meters per second (from -5.0 to 5.0); rod angle in radians (from -0.5 to 0.5 with respect to the vertical) and rod angular velocity in radians per second (from -5.0 to 5.0).
- Two hidden layers, 4 and 2 neurons each.
- One output. The neurons used in this neural network could only provide output in the range from 0.0 to 1.0 , which is later scaled to the range from 0.0 to 5.0 (motor control voltage).

The neural controller has been subjected to a period of genetic optimization through the SAFE-LEARNING method described in [6]. The optimization goal was to produce a neural controller (LEARNING controller) that has a better steady state performance (expressed in the terms of RMS error of the cart position and rod angle during rod balancing) than the original SAFE controller. Due to the nature of the failure-free learning method, the training process was limited to a closed neighborhood (further denoted as Ω_{SAFE}) surrounding the regulation point. The neural controller never observed state variables exceeding the boundaries of Ω_{SAFE} , and, therefore, cannot be used outside of that region. The optimization process emphasized optimization of the cart position RMS or rod angle RMS through utilization of the weight coefficients P_w (position weight coefficient in meters)

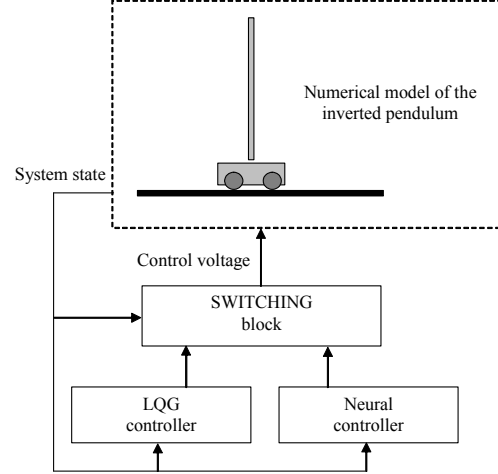


Fig. 1: Block-diagram of the hybrid controller.

and A_w (angle weight coefficient in degrees) in the fitness function F of GA.

$$F = \int_0^T \left(\frac{P(t)}{P_w} \right)^2 + \left(\frac{A(t)}{A_w} \right)^2 dt, \quad (2)$$

where $P(t)$ is cart position in meters, $A(t)$ is rod angle in degrees. Average cart position and rod angle RMS of the inverted pendulum system controlled by the neural controllers optimized with different coefficients P_w and A_w are listed in Table 1. The neural controller optimized with equal importance of the cart position and rod angle was chosen to be used in the hybrid controller.

Also, it is noted that all of the neural controllers optimized by GA produced bang-bang type of control, in contrast to the continuous output of the LQG controller.

The SAFE controller in the SAFE-LEARNING method is a controller that has been validated for performance and stability of operation, though it might not be an optimal controller. The SAFE controller provides a control design, which is ensured to be failure-free even in cases in which the GA optimization process may generate unacceptable solutions. The same LQG controller has been used both as the SAFE controller during optimization and as a part of the hybrid controller.

Table 1: The average RMS of cart position and rod angle obtained on the neural controllers optimized with different weight coefficients P_w and A_w . Relative improvement in RMS is given in comparison to the LQG controller.

#	P_w , centimeters	A_w , degrees	Cart position RMS, centimeters	Rod angle RMS, degrees	Reduction in cart position RMS, %	Reduction in rod angle RMS, %
1	0.5	2.0	0.6527	0.6431	53.07	9.83
2	0.5	1.0	0.6553	0.6131	52.89	14.04
3	0.5	0.5	0.692	0.5705	50.25	20.01
4	1.0	0.5	0.7759	0.5048	44.22	29.22
5	2.0	0.5	0.8508	0.4795	38.83	32.76

The switching block monitors the state of the controlled system and switches control from the LQG controller to the neural controller and back. The suggested principle of operation for the switching block is illustrated in Fig. 2. The system starts at some initial state S_{INIT} , with the LQG controller in control of the system. After a transient process, the system state becomes sufficiently close to the regulation point S_0 . Subspace Ω_N defines the region where the current state of system is considered to be close enough to S_0 , so that the control can be turned over to the neural controller. The neural controller assumes control of the system and continues it until the system state exceeds boundaries of the region of normal operation Ω_L . This event may be the result of changing the reference point of the regulation process. Given such an event, the control is turned over to the LQG controller until the transient process is complete.

The switching block is probably the most important part of the hybrid controller. The quality of the regulation process depends upon timely switching from LQG to neural controller when the current state is within Ω_N . The system's performance will be unacceptable if the switching from the neural to the LQG controller is too late and the LQG controller is not able to recover when the system state transitions outside of Ω_L .

Practical issues related to the implementation of the suggested method include (but are not limited to) a reliable

definition of the regions Ω_N and Ω_L . Region Ω_N should correspond to the steady state mode of operation for the LQG controller. The switching block should turn control over to the neural controller only during steady state operation, but not during a transient process. Region Ω_L should correspond to the steady state mode of operation for the neural controller, which may or may not be equal, smaller or larger than Ω_N . Size of the subspace Ω_L is a result of genetic optimization of a neural controller and will vary depending on the optimization goals. However, region Ω_L (and Ω_N) should always be a subspace of the region Ω_{SAFE} in which the neural controller was optimized:

$$\begin{cases} \Omega_L \subset \Omega_{SAFE} \\ \Omega_N \subset \Omega_{SAFE} \end{cases} \quad (3)$$

Both region Ω_N and region Ω_L can be experimentally established by observing balancing on the inverted pendulum system by the LQG and the neural controller, respectively. The actual definition of the regions may be obtained as:

1. A neural network mapping the region of steady state operation.
2. A statistical mapping, such as a clustering technique.
3. An enclosing hypercube or a hypersphere.

The hypercube approach is the simplest but the least accurate of those listed. The hypercube mapping was selected for use in the hybrid controller due to simplicity of implementation. Further development of the hybrid controller will include improved mapping techniques.

The boundaries of the hypercube can be easily obtained by observing the steady state operation of a controller for a sufficiently long period of time. Fig. 3 illustrates histograms of the cart position, cart velocity, rod angle and rod angular velocity for the LQG and for the neural controller during an operation period of 1000 seconds. The hypercube region for switching from the LQG to the neural controller Ω_{NHC} is specified by the switching limits with respect to the regulation point S_{REG} . However, being a crude approximation of the Ω_N , a hypercube may also include states that can only be observed during a transient process. A possible solution to this problem is to monitor the state transitions of the system in time and perform switching from the LQG to the neural controller only after a period of time T_{SW} that system spends in the region Ω_{NHC} . Such a switching mechanism reflects on the properties of the transient processes, which will transition through Ω_{NHC} in a relatively short time, while a steady state process should remain inside Ω_{NHC} indefinitely. The hypercube region for switching from the neural to the LQG controller Ω_{LHC} is defined similarly to Ω_{NHC} . Being an imprecise approximation of Ω_L , Ω_{LHC} may create situations, where switching from the neural to the LQG controller is performed late, reducing the quality of control. However, as long as $\Omega_{LHC} \subset \Omega_{SAFE}$, the system should remain stable during the transition.

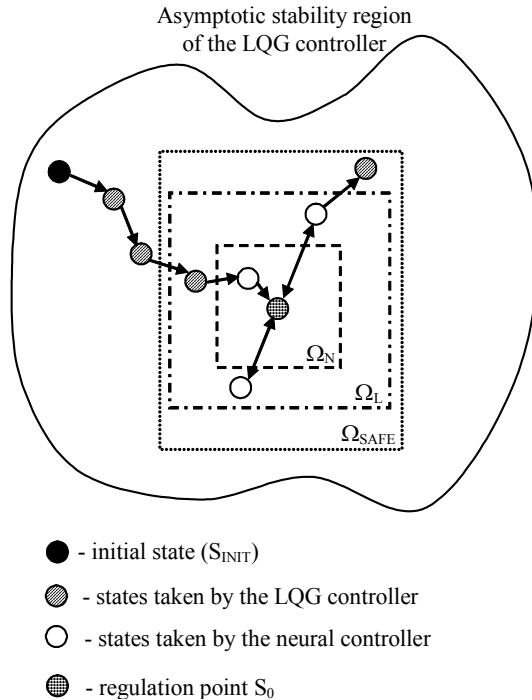


Fig. 2: A two dimensional example of the switching block operation

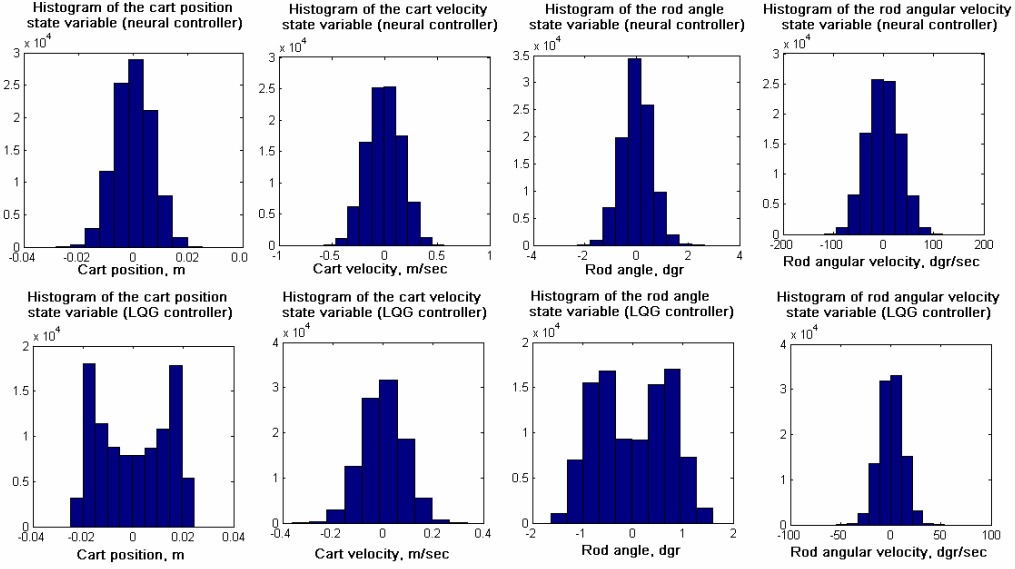


Fig. 3: Two-dimensional projections of system variables during 30-second balancing by a neural controller

The flowchart of the switching algorithm is presented in Fig. 4.

IV. RESULTS

Several experiments were conducted with the different parameters of the reference signals. The hypercube boundaries were established from the histograms shown in Fig. 3. The boundaries were established as a range containing 99% of the observed values. The following numerical experiments were conducted for the LQG and for the hybrid controller:

1. Balancing the pole with the initial conditions close to zero.
2. Balancing from non-zero (cart offset 0.15 m) initial conditions.
3. Tracking a low-frequency (frequency 0.05Hz, amplitude 0.15 m) square wave.
4. Tracking a high-frequency (frequency 0.5Hz, amplitude 0.15 m) square wave.

The average RMS of the cart position and pole angle of the inverted pendulum system obtained during a 100-second run period are listed in Table 2.

As expected, the hybrid controller offered the best improvement in the quality of control for the balancing problem with initial conditions close to zero. The system almost immediately switches control to the neural controller, which takes control for the remaining time.

Similar to the first experiment, the hybrid controller offered significant improvement for the case of non-zero initial conditions. However, for the third experiment, the

hybrid controller provided poorer performance than the stand-alone LQG controller. Such an effect may appear due to frequent switching from the LQG controller to the neural controller and back in a system with coarse approximation of Ω_N and Ω_L . Finally, experiment number four did not demonstrate any improvement over the stand-alone LQG controller. Such a result was expected as the hybrid controller stays switched to the LQG during the transient processes.

Fig. 5 illustrate operation of the hybrid controller for the experiment with the 0.05 Hz square wave.

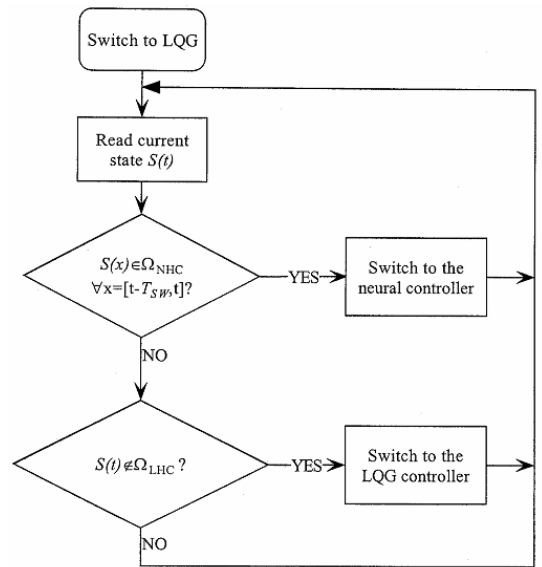


Fig. 4: Flowchart of the switching algorithm

Table 2: The average RMS of cart position and rod angle obtained on the stand alone LQG and the hybrid controllers.

Controller	Parameter	Balancing with zero initial conditions	Balancing with 0.15 m initial cart offset	Tracking 0.05 Hz square wave	Tracking 0.5 Hz square wave
LQG	Cart position RMS, m	0.014	0.019	0.077	0.20
	Rod angle RMS, dgr	0.72	0.75	1.55	4.03
Hybrid	Cart position RMS, m	0.0064	0.016	0.095	0.20
	Rod angle RMS, dgr	0.56	0.62	2.29	4.03

V. CONCLUSIONS

The hybrid controller, described in this paper, has shown certain advantages over conventional LQG controller:

1. A neural controller, trained directly on the controlled system, accounts for the existing non-linearities and uncertainties of the parameters, improving quality of control.
2. As a part of the hybrid, the LQG controller provides a much wider region of operation than the neural controller alone and ensures stability of the system operation during transient processes.
3. Conducted experiments have shown that the hybrid controller outperforms the stand-alone LQG controller for a variety control tasks.

The coarse switching mechanism used here has demonstrated feasibility of the hybrid controller approach, but lacks robustness. Further research is necessary to completely develop the functioning of the switching block in

order to provide the best quality of control and stability of the hybrid controller.

VI. ACKNOWLEDGEMENTS

The authors wish to acknowledge the support provided for this work by Allegheny Power and the simulation model designed by Dr. Diego DelGobbo.

VII. REFERENCES

- [1] M. Randall, "The Future and Applications of Genetic Algorithms", *Proceedings of the Electronic Directions to the Year 2000 Conference*, IEEE Computer Society Press, March, 1995, Adelaide, pp. 471 – 475.
- [2] D. Dasgupta and D.R. McGregor, "Genetically designing neuro-controllers for a dynamic system," in *IJCNN'93*, 1993, pages 2951—2954.
- [3] M.G. Cooper and J.J. Vidal, "Genetic design of fuzzy controllers," in *Proceedings of 2nd International Conference on Fuzzy Theory and Technology*, 1993.
- [4] M.M. Chowdhury and Yun Li, "Evolutionary Reinforcement Learning for Neurofuzzy Control," in *Technical Report, CSC-96020*, Faculty of Engineering, Glasgow G12 8QQ, Scotland, UK, 1997
- [5] H. Shimooka and Y. Fujimoto, "Generating Equations with Genetic Programming for Control of a Movable Inverted Pendulum", in *Second Asia-Pacific Conference on Simulated Evolution and Learning*, 1998, Australian Defense Force Academy, Canberra, Australia.
- [6] E.S. Sazonov, D. Del Gobbo, P. Klinkhachorn and R. L. Klein, "Failure-Free Genetic Algorithm Optimization of a System Controller Using SAFE/LEARNING Controllers in Tandem", *Proceedings of 34th Southeastern Symposium on System Theory (SSST)*, Huntsville, AL, March 2002, pp.287-292
- [7] D. Del Gobbo, "Sensor failure detection and identification using extended Kalman filtering", MS thesis submitted to West Virginia University, 1998.

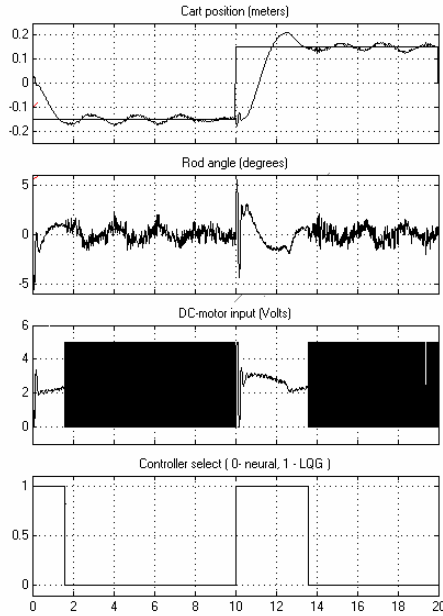


Fig. 5: Cart position, rod angle, motor control voltage and controller select signal acquired from the hybrid controller during a balancing experiment with non-zero initial conditions